Bioconjugate Chemistry

Article

pubs.acs.org/bc

Directed Polyvalent Display of Sulfated Ligands on Virus Nanoparticles Elicits Heparin-Like Anticoagulant Activity

Griffin Mead, Megan Hiley, Taryn Ng, Conrad Fihn, Kevin Hong, Myles Groner, Walker Miner, Daniel Drugan, William Hollingsworth, and Andrew K. Udit*

Department of Chemistry, Occidental College, Los Angeles, California 90041, United States

Supporting Information

ABSTRACT: Heparin is a sulfated glycosaminoglycan that is widely used as an anticoagulant. It is typically extracted from porcine or bovine sources to yield a heterogeneous mixture that varies both in molecular weight and in degree of sulfation. This heterogeneity, coupled with concern for contamination, has led to widespread interest in developing safer alternatives. Described herein are sulfated bacteriophage Qβ virus-like particles (VLPs) that elicit heparin-like anticoagulant activity. Sulfate groups were appended to the VLP by synthesis of single- and triple-sulfated ligands that also contained azide groups. Following conversion of VLP surface lysine groups to alkynes, the sulfated ligands were attached to the VLP via copper-catalyzed azide−alkyne cycloaddition (CuAAC). MALDI-MS analysis of the intermediate alkyne VLP indicated that the majority of the coat proteins contained 5−7 of the alkyne linkers; similar analysis of the intermediate alkyne particles conjugated to a fluorescein azide suggest that nearly the same number of attachment points (3−6) are modified via CuAAC. Analysis by SDS-PAGE with fluorescent staining indicated altered migration patterns for the various constructs: compared to the wild-type nanoparticle, the modified coat proteins appeared to migrate farther toward the positive pole in the gel, with coat proteins displaying the triple-sulfated ligand migrating significantly farther. Clotting activity analyzed by activated partial thrombin time (APTT) assay showed that the sulfated particles were able to perturb coagulation, with VLPs displaying the triple-sulfated ligand approximately as effective as heparin on a per mole basis; this activity could be partially reversed by protamine. ELISA experiments to assess the response of the complement system to the VLPs indicate that sulfating the particles may reduce complement activation.

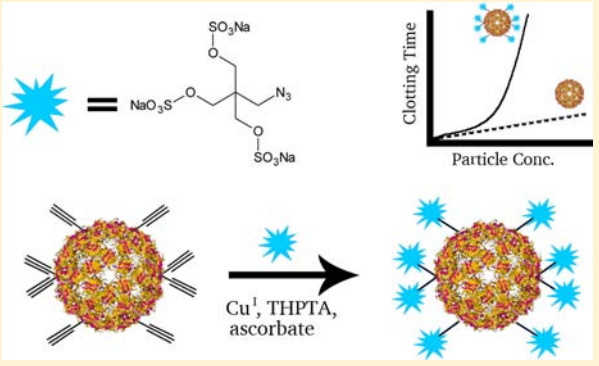

INTRODUCTION

Heparin is a naturally occurring glycosaminoglycan (GAG) of variable molecular weight (5−30 kDa) and sulfation density, composed of repeating units of uronic acid and glucosamine arranged in linear chains on a core protein.[1,2] Unfractionated heparin (UFH) is purified from porcine or bovine tissue as a heterogeneous mixture of polymers with an average molecular weight of ∼12 kDa.[3,4] UFH has been utilized as an anticoagulant since the 1940s and remains broadly used today,[5] especially during cardiac procedures, and for arterial and venous thromboembolism.[6,7] UFH functions as an anticoagulant by acting as a cofactor for several serine protease inhibitors in the inactivation of coagulation serine proteases;[8] the most significant of these is the inactivation of proteases factor Xa (FXa) and thrombin by antithrombin (AT). A specific pentasaccharide in the heparin polymer binds with high affinity and causes a conformational change that activates AT,[9] which in turn stimulates inactivation of FXa by AT. Thrombin, however, is only inactivated when the heparin chain is also long enough to bind both AT and thrombin through a specific heparin binding site on thrombin,[10] thus constraining AT and thrombin together on one heparin chain.

Despite its clinical ubiquity[7] the heterogeneity of UFH presents significant challenges for use. Most notably, bleeding complications with UFH treatment are substantial: for example, of Medicare patients in 2004, 350 000 people nationwide had adverse heparin events, 5% of which were life threatening.[11] Use of UFH can lead to heparin-induced thrombocytopenia, characterized by enhanced platelet aggregation via a non-immune (Type I, ∼5−30% of patients) or immune-mediated pathway (Type II, ∼1−3% of patients).[12] UFH's heterogeneity is also a complicating factor for individuals displaying heparin resistance, with reported incidences as high as 20% of treated patients.[13] Thus, the variability in patient response to UFH and the resulting complex pharmacokinetic profile demands careful monitoring of individuals during treatment.[14] Adding to the problems of naturally derived heparin is the potential for contamination with closely related GAGs: in 2007, several deaths resulted from patients being administered heparin preparations that were contaminated with the structurally

Received: May 3, 2014
Revised: June 21, 2014
Published: June 24, 2014

dx.doi.org/10.1021/bc500200t | Bioconjugate Chem. 2014, 25, 1444−1452

Scheme 1. Synthetic Routes for Ligands 1 and 2

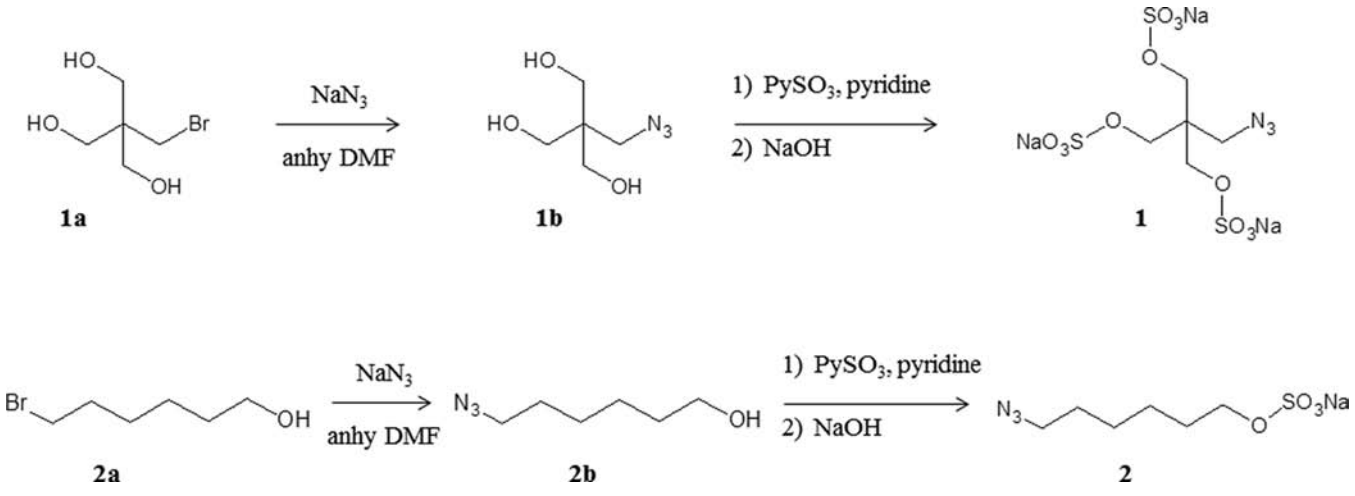

Scheme 2. Bioconjugation Scheme[a]

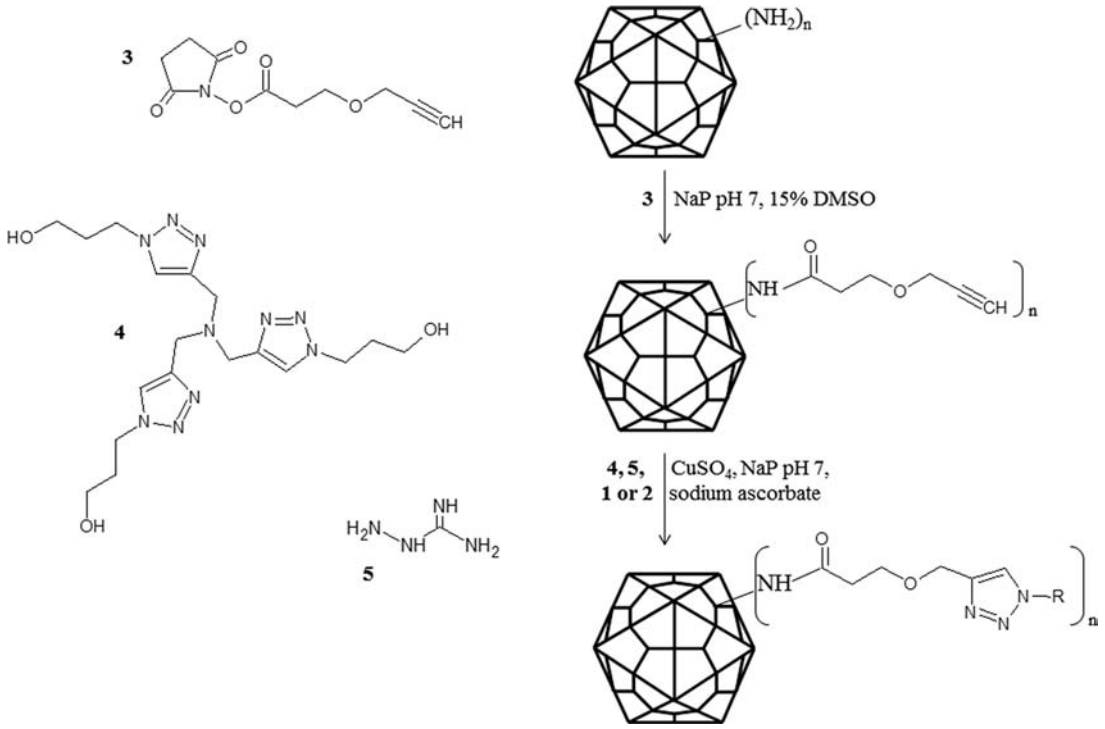

[a]The first step converts lysine residues to alkynes for subsequent CuAAC reaction with ligands **1** or **2** (R groups), which have azides.

similar chondroitin sulfate.[15,16] More recently it has been shown that, depending on the sulfation pattern ("sulfation code"[17]), heparin has varied physiological effects beyond hemostasis that include roles in carcinogenesis and cell signaling.[1,18−23] Thus, heparin's heterogeneity may also lead to unwanted off-target effects when used clinically.

The challenges associated with clinical use of UFH have led to the development of possible alternatives.[24,25] Low molecular weight heparins (LMWH, ~6000 Da) derived from chemical or enzymatic degradation of heparin benefit from displaying more predictable dosing responses and have thus played an increasingly prominent clinical role in preventing thrombosis, although their longer half-lives and lack of fully effective reversal agents (e.g., protamine) are problematic.[6,13,26−32] Alternatively, there is currently much research aimed at developing synthetic heparins.[33] Some investigators have been successful at partially reproducing sulfated GAG-like activity with scaled down oligosaccharides using elegant (although daunting) syntheses.[17,34−38] For example, chemical synthesis of Arixtra, a successfully marketed ultralow molecular weight heparin (ULMWH) pentasaccharide (1508 Da), requires upward of 50 steps and yields below 1%.[39−41] More recently reported chemoenzymatic synthetic schemes for ULMWHs fare better (30−40% overall yield), although still onerous (10−12 steps, mg scale) with the additional caveat of requiring substrates that are recognized by the enzymes.[42,43] Notably, for all of these compounds, fully effective reversal agents are still lacking, an important consideration that should be factored into designing a heparin alternative. (Note that non-GAG small

dx.doi.org/10.1021/bc500200t | Bioconjugate Chem. 2014, 25, 1444−1452

molecule anticoagulants have also been developed, e.g., dabigatran, argatroban. See Schulman[25] for some discussion.)

In general, challenges for synthetic heparins include biodegradability, targeted modifications to vary the number and position of sulfate groups, and ease of synthesis. Thus, desired characteristics for potential heparin synthetics include a biomimetic scaffold that may resemble native GAG structures while also being biodegradable, a polyvalent structure to exploit the low affinity–high avidity interactions typical of biological systems, and precise control over the sulfated ligands presented. To address these challenges, the work herein describes chemically tailored virus-like particles (VLPs) using bacteriophage Qβ as a platform for polyvalent display of sulfation patterns that may act similarly to heparin. Qβ is 28 nm in diameter with icosahedral symmetry, composed of 180 identical copies of a 133 amino acid coat protein.[44] In addition to fulfilling the criteria outlined above for potential heparin alternatives, viruses are good candidates for biomedical applications given that they are designed (by nature) to interact with physiological targets. Perhaps most attractive is the particle's programmed self-assembly, which reliably generates scaffolds for polyvalent presentations using a repeating peptide structure that is readily modified via mutagenesis. Qβ in particular has been amenable to both chemical modification and mutation, and several potential biomedical applications based on the Qβ scaffold have been investigated.[45−50] Indeed, prior work with Qβ demonstrated that mutant VLPs displaying additional positive charges could act as potent heparin antagonists, providing a potential alternative to protamine.[46,51]

RESULTS AND DISCUSSION

Synthesis of Sulfated Ligands. Scheme 1 depicts the synthetic routes used to generate the sulfated ligands. The ligand scaffolds were chosen to provide a potentially wide range of activity while still being relatively straightforward to synthesize from readily available starting materials. In addition, azides were installed to exploit copper-catalyzed azide–alkyne cycloaddition (CuAAC) for subsequent bioconjugation.[52−54] **1** provides a high charge density with likely limited conformational flexibility due to steric hindrance and electrostatic repulsion. By contrast, **2** should be far more flexible, thus allowing it to find optimal configurations to interact with potential binding partners. Scheme 1 shows that similar synthetic methodologies can be used for each ligand, resulting in sodium salts which showed good stability (stored on the benchtop at room temperature for months without degradation). Characterization by NMR, IR, and ESI-MS were used to confirm the identity of the products (see Supporting Information, Figures S1–S6). Notably, purification of the pyridine-sulfur trioxide sulfating agent to remove any sulfuric acid produced from hydrolysis was critical for achieving clean products in good yields (see Experimental Procedures for details).

Bioconjugation. The bioconjugation strategy is shown in Scheme 2. The initial approach focused on targeting **1** and **2** to surface lysine residues following modification of the side chains with *N*-hydroxysuccinimide (NHS) esters. Wild-type Qβ has three surface, highly solvent-exposed lysine residues: K2, K13, and K16 (the computationally derived relative solvent-accessibility profile is shown in SI Figure S7). Figure 1 is a representation of the Qβ coat protein derived from the crystal structure, highlighting these three lysine groups. The remaining four lysines in the coat protein face the interior of the capsid. Spherical viruses use interior-facing cationic residues to bind RNA,[55] with a specific hairpin in Qβ binding native genetic material;[56,57] thus, the internal lysines are likely not readily modified. In addition to the surface lysines, the N-terminal amine is also accessible (and immediately adjacent to K2), and prior work has shown this to be a viable attachment point.[58] Thus, there are four potential surface residues that can serve as targets for modification by NHS ester reagents.

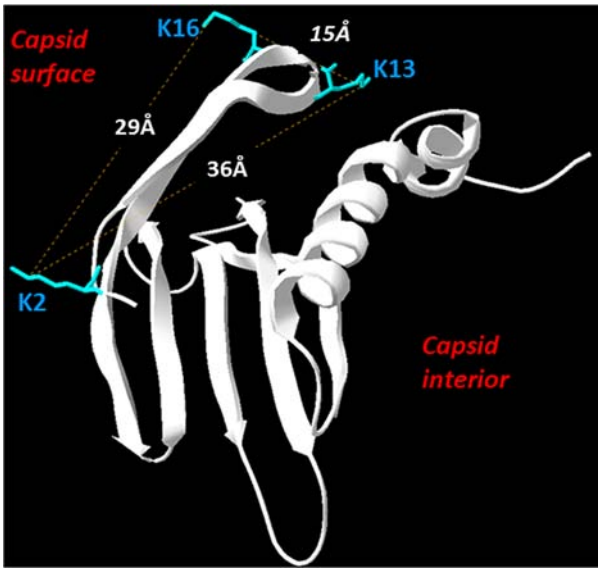

Figure 1. Representation of the Qβ coat protein showing the three surface lysine groups targeted for modification with **3**. The N-terminal amine lies close to K2.

Reaction of Qβ with **3** to generate the intermediate alkyne-derivatized particle (Scheme 2) was carried out on the benchtop at room temperature overnight. With all 7 lysines and the N-terminal amine taken into account, the reaction contained a 25-fold excess of **3** per amine to promote complete reaction of surface amines. MALDI-MS analysis (SI Figure S8) revealed multiple peaks, which are presented in Table 1. Both

Table 1. Summary of Peaks Observed in the MALDI-MS Spectrum of VLP-3, the Intermediate VLP Displaying Alkyne Groups

# alkyne linkers	calcd M	obsd $M+H^+$	obsd $M+Na^+$
4	14563		14588
5	14673	14674	14698
6	14783	14784	14807
7	14893	14894	14919
8	15003	15011	

H^+ and Na^+ adducts were detected, with adjacent peaks corresponding to the same cation adduct approximately separated by the mass equivalent of the added alkyne linker group (110 m.u.). The data suggest that at least four alkyne linkers were added per coat protein, with the majority (by integration) containing 5–7 of the added groups. This indicates that some internal lysines were also modified, which is unsurprising given the large excess of **3** used. The reaction was purified by ultracentrifugation and resuspension of the pelleted virus in 0.1 M sodium phosphate (NaP) pH 7 buffer for subsequent attachment of the sulfated ligands.

CuAAC reactions (Scheme 2) were carried out according to Hong with a few modifications.[52] The concentration of sulfated ligand in the reactions was markedly higher at 40 mM (cf. μM concentrations), which was found to be optimal for this system. Reactions were also performed in an oxygen depleted atmosphere (i.e., not strictly anaerobic) to minimize generation of reactive oxygen species through dioxygen reduction by ascorbate; greater yields were observed for this system in a reduced oxygen environment. Purification was achieved by ultracentrifugation to pellet the particles, which were resuspended in HBS (50 mM HEPES, 100 mM NaCl, pH 7.4) for use in subsequent clotting assays. The integrity of the particles was analyzed by size exclusion chromatography, which yielded elution profiles for the sulfated VLPs that were similar to the unmodified particle (large peak early in the run due to rapid elution of the relatively large nanoparticle; see SI Figure S9 for FPLC). Notably, for particles displaying ligand **1** the elution profile has an additional feature at 24 min; while it is not clear what this may represent—particles interacting with the resin, aggregates, etc.—it does not correspond to disassembled particles as the individual coat proteins are not readily soluble.[59] (FPLC of Qβ thermally denatured in the presence of MES-SDS buffer and DTT yielded only a weak signal at 29 min; data not shown.)

Figure 2 displays results from SDS-PAGE analysis of the various Qβ constructs. The sulfated particles were too dilute for

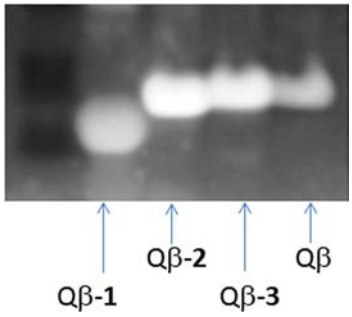

Figure 2. SDS-PAGE of Qβ coat proteins. The gel was stained with the fluorescent SYPRO stain and visualized with UV light. Qβ-**1** and Qβ-**2** have ligands **1** and **2**, respectively, appended to them via linker **3**, Qβ-**3** has only linker **3**, and Qβ is the unmodified wild-type coat protein (14.1 kDa).

Coomassie staining; thus, the gel was stained using the SYPRO reagent (a ruthenium dye). The gel was visualized by fluorescence of the stained protein under a UV lamp. The image in Figure 2 shows that the wild-type (14.1 kDa) and alkyne-modified particles appear to migrate similarly; however, the sulfated particles show different migration patterns. Particles modified with **2** appear to migrate slightly farther down the gel, while particles with **1** are markedly shifted relative to the wild-type. These shifts may have to do with the added negative charge on the particles, causing them to migrate farther toward the positive pole of the gel. The fact that particles with **1** migrate farther than particles with **2** serves to underscore the electrostatic effect of the triple-sulfated **1** compared to the monosulfated **2**. Attempts to further investigate particle surface charge using anion exchange chromatography with DEAE-sepharose proved intractable for unknown reasons.

MALDI-MS of the sulfated particles failed to produce sufficiently intense signals to definitively quantify the number of ligands on the VLPs. The added sulfate groups may affect ionization or interact unfavorably with the matrices used, or they may be poorly compatible with the work-up conditions for the coat protein (see Experimental Procedures for details). As a proxy, the intermediate VLP-alkyne particle was subjected to CuAAC reaction with a fluorescein azide (see SI Figure S9 for FPLC), the product of which was amenable to analysis by MALDI-MS (SI Figure S10). The data indicate that the majority of the coat proteins contained three to six fluorescein molecules, suggesting that bioconjugation efficiency via CuAAC was high. Given the large hydrophobic structure of fluorescein it is reasonable to assume that bioconjugation of the smaller sulfated ligands would be at least as efficient as the fluorescein reaction. Comparing quantification by MALDI-MS with absorption of fluorescein ($\varepsilon_{495\ nm} \sim 70\ mM^{-1}\ cm^{-1}$) yielded a poor correlation, presumably due to an altered extinction coefficient when the molecule is conjugated close to the VLP surface (Strable et al.[58] discuss some of the issues related to conjugation of fluorescein to VLPs).

Clotting Assays. The activated partial thrombin time (APTT) assay was used to evaluate the ability of the sulfated particles to perturb coagulation. Assays were conducted with the Stago STart 4 hemostasis analyzer in APTT mode, which records the time taken for a liquid sample to reach a viscous gel-like state (i.e., when coagulation is achieved). Samples contained a mixture of normal human plasma, a platelet surrogate (Platelin), and the reagent of interest (VLP, heparin) in HBS buffer (using phosphate buffer causes calcium in the reaction to precipitate). The resulting data are shown in Figure 3; the *y*-axis is plotted in terms of relative clotting time to

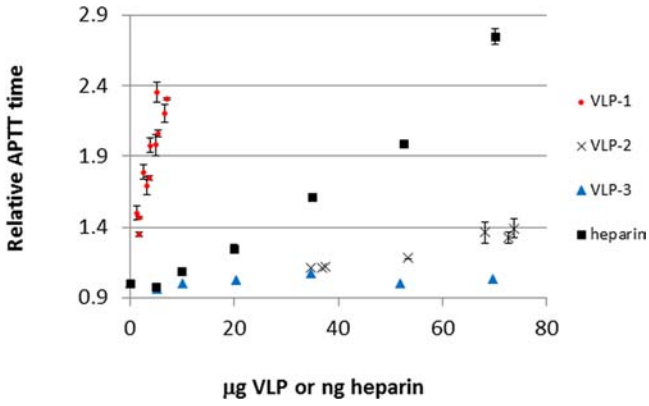

Figure 3. APTT assay. Relative times are based on normal clotting time; for example, a value of 2 represents a trial that took twice as long to clot compared to the control (~40 s). Note that in the case of heparin (square points) the *x*-axis represents nanograms of added heparin. Error bars reflect a minimum of two trials.

facilitate comparisons between different lots of plasma (e.g., a value of 2 indicates that clotting takes twice as long compared to normal clotting). Under the assay conditions used, normal clotting takes approximately 40–45 s, while clotting reactions that go beyond 130 s in the presence of anticoagulants typically yield highly variable data. Notably, while the *x*-axis is in terms of micrograms of VLP added to the clotting reaction, for the heparin reactions the values represent nanograms of added heparin. All reactions were performed at least in duplicate.

As a positive control, heparin was first evaluated in the APTT assay. The potency of heparin as anticoagulant can be clearly seen in Figure 3, with 70 ng yielding clotting times that

dx.doi.org/10.1021/bc500200t | *Bioconjugate Chem.* 2014, 25, 1444–1452

approach three times the normal value. The corresponding negative control, the unsulfated VLP-alkyne intermediate, showed virtually no effect on clotting even at 70 μg of added particle (this agrees with a prior study[46,51] that evaluates various Qβ constructs as heparin antagonists). Controls using the bare, unconjugated ligands in the assay showed no effect on clotting (evaluated up to 275 μg of added ligand, not shown). In contrast to the VLP-alkyne negative control, the sulfated particles showed anticoagulant activity, but to a significantly differing degree that appears to track with the valency of the different ligands. The slopes of the lines, representing relative activity per microgram of added VLP and thus providing a measure of relative potency, differ by a factor of 23.

While VLP-**1** appears quite potent, this is only achieved at microgram levels whereas heparin is active at nanogram quantities. However, while 3 orders of magnitude apart on a mass basis, the calculation on a molar basis is more favorable. Figure 3 shows that 52.5 ng of heparin (~12 kDa) has APTT activity equivalent to 5 μg of VLP-**1** (~2.6 MDa): this corresponds to approximately 4 pmol of heparin and 2 pmol of nanoparticle.

Protamine titrations were also performed in the APTT assay to determine if the anticoagulant activity of the potent VLP-1 could be attenuated (SI Figure S11). Assays conducted with plasma containing 2.6 μg of VLP-1 (1 pmol VLP) had a relative clotting time of 1.8; this was reduced to 1.4 between 10 and 15 μg (2−3 nmol) of added protamine, while the addition of more protamine caused a sharp increase in clotting time (as expected for protamine overdose;[60,61] SI Figure S12). Thus, protamine does appear to have some capability of antagonizing the activity of VLP-1, although the activity is not fully reversible, which is in contrast to the protamine−heparin interaction (SI Figure S12). The polyvalent nature of the particle likely permits multiple protamine peptides to bind the VLP; however, electrostatic repulsion between adjacently bound protamine may limit this interaction, thereby preventing full inhibition of VLP activity.

The APTT assay is both reliable and broadly used clinically; however, it does not give any indication as to which components in the coagulation cascade may be antagonized by the VLP. While a full investigation into the mechanism is beyond the scope of this study, a preliminary experiment was performed using the HEPtest clotting assay which tests for the ability of heparin to catalyze the inactivation of exogenous factor Xa by antithrombin. Data were collected for both VLP-1 and VLP-2 using quantities that gave strong responses in the APTT assay. The data (SI Figure S13) appear to indicate that there is a minimal effect of the VLPs on FXa activity; however, the mild response of heparin in this assay and the significant scatter observed for the VLP constructs suggest that further investigations are warranted.

Complement Activation. Nanoparticles are known to activate the complement system;[62] however, heparin is an inhibitor of complement activation through various mechanisms.[63] To explore the effect of the VLPs on the complement pathway, ELISA assays were performed to test for formation of the terminal complement complex (TCC) which results if any of the classical, lectin, or alternative pathways are activated. Prior work using this assay has suggested that a 2−4-fold increase of the TCC concentration compared to the baseline value is considered to represent an increased risk of hypersensitivity reactions, while values above this range indicate a high risk.[64] The data shown in Figure 4 are plotted relative to the amount of TCC detected in the absence of VLP. Within the

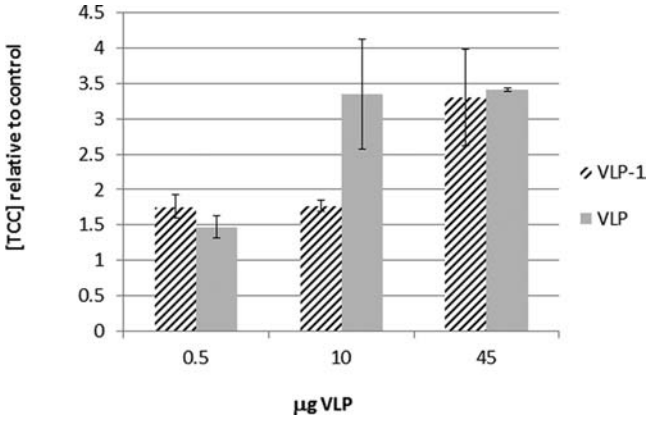

Figure 4. ELISA complement assay. The *y*-axis represents the concentration of the terminal complement complex (TCC) measured relative to a control sample containing no VLP. Error bars reflect a minimum of two trials. A sample containing *E. coli* cell lysate, anticipated to be a strong activator of complement, yielded a relative [TCC] of 4.07.

0.5−10 μg range where VLP-1 is effective in the APTT assay there appears to be a less than 2-fold increase in TCC levels, whereas the unmodified VLP showed significant complement activation at 10 μg. (For comparison, *E. coli* cell lysate yielded a relative TCC concentration of 4.07.) The ligands on VLP-1 may partially mask the particle from complement activation, similar to what is known to occur with PEG coatings.[62]

■ SUMMARY

The emergence of compounds with heparin-like activity based on alternative scaffolds has shown some promise: examples include sulfated dextrans that stimulate tissue regeneration and display antithrombotic activity,[65] and polystyrenesulfonates that activate basic fibroblast growth factors,[66] with the latter representing a far simpler structure than the native GAG. Dendrimer structures have also seen good success[67] and likely represent a more appropriate comparison to the VLP nanoparticle scaffold described here. With specific focus on anticoagulant activity, previous work described the synthesis of terminally sulfated polyglycerol dendrimers which displayed APTT activity that was 5−8% that of heparin.[68]

Herein it has been demonstrated that polyvalent display of sulfated moieties on a virus nanoparticle scaffold can elicit heparin-like anticoagulant activity. Followup investigations will focus on the mechanism of action. In comparison to heparin, the VLP scaffold is rigid; thus, inhibition of coagulation is not likely to occur via interaction of the sulfated VLP with thrombin which requires that, in the case of heparin, both thrombin and antithrombin be adjacently bound. Regarding FXa activity, while the HEPtest assay was not conclusive, alternative assay formats (e.g., chromogenic) may prove informative. Also, additional biophysical studies (e.g., SPR) can potentially elucidate specific binding partners for the sulfated VLPs.

Ultimately the VLP serves as a versatile, malleable tool that can be used to shed light on both the mechanism and activity of possible heparin alternatives. Unlike dendrimers where ligand positioning can be difficult to control, the VLP coat protein can be readily and reliably mutated to generate nanoparticles with varied number and spacing of ligand attachment points. Thus, the effect of sulfation pattern can be readily explored. Further,

the size of the VLP can be varied, either by making "mini-Qβ" particles[59] or using an entirely different scaffold (e.g., hepatitis B virus[69]). Exploring ligands more similar to native GAG structures (e.g., glucose derivatives) provides yet another possibility to diversify the VLP construct. Such diversity provides an opportunity to generate a selective nanoparticle that preferentially interacts with components in the coagulation cascade; for example, the known interaction that heparin has with AT can potentially be modeled onto the VLP surface to create a potent and selective polyvalent AT-binding particle.

EXPERIMENTAL PROCEDURES

3-Prop-2-ynyloxy-propionic acid 2,5-dioxo-pyrrolidin-1-yl ester (**3**) and tris(3-hydroxypropyltriazolylmethyl)amine (THPTA, **4**) were purchased from Click Chemistry Tools. Heparin was purchased from Sigma (H3393, 198 USP units/mg). All other reagents were purchased from Fisher Scientific and VWR unless otherwise stated.

Protein concentrations were determined by modified Lowry assay (Fisher), except for the sulfated VLPs which were quantified using the Bradford assay (Fisher). Using the Lowry assay for the sulfated particles gave inordinately high values for the protein concentration, which was corroborated via protein gel and quantitative staining with the SYPRO reagent (see below). Presumably the added sulfate groups interfered with the assay.

VLP Expression and Purification. Wild-type VLPs were expressed using the pQE-60 plasmid (Amp resistance) harboring the gene for the coat protein (133 amino acids) in *E. coli* methionine auxotroph cells (Kan resistance) kindly provided by the Tirrell lab (Caltech). A non-auxotroph strain could also be used, but we have consistently produced high yields with this system and so continue to use it.

Five milliliter overnight cultures of each VLP in SOB media (Fisher) at 37 °C with the appropriate antibiotics were diluted the following morning 100-fold into MDG media supplemented with 100 mg of methionine per liter of culture. MDG media was made exactly as described.[70] Four hours post-dilution, IPTG was added to each culture to a final concentration of 1 mM. After growing for an additional 8 h at 37 °C, the cells were harvested by centrifugation (4000 rpm for 10 min at 4 °C, Beckman JA-10 rotor) and the pellets stored at −20 °C.

The following protocol was applied to cell pellets derived from 500 mL of media. The pellets were thawed on the benchtop for 10 min and then resuspended in 30 mL of 50 mM sodium phosphate (NaP) pH 7 buffer. One milligram each of DNase, RNase, and lysozyme were then added, and the pellets were left on the benchtop with occasional swirling for 10−15 min. The mixture was then sonicated on ice with a 30% duty cycle, ∼1 min per round of sonication until the mixture was fluid (typically 3−5 rounds). The mixture was then centrifuged at 4 °C for 15 min at 14 000 rpm using a JA-17 rotor. To the supernatant, an equal volume of a 1:1 $CHCl_3$:*n*-butanol solution was added, mixed thoroughly, and then centrifuged at 1000 rpm for 2 min using a tabletop centrifuge to separate the layers. The top aqueous layer was recovered, and to this ammonium sulfate was added, approximately 8 g per 30 mL of solution (0.265 g/mL). The mixture was placed on a rotator in the fridge (4 °C) for at least 1 h, followed by centrifugation at 14 000 rpm for 15 min using a JA-17 rotor. The supernatant was carefully discarded, and the pellet resuspended with 2−3 mL of 50 mM NaP pH 7 buffer. The solution was then centrifuged again using a JA-17 rotor at 14 000 rpm for 15 min, and the supernatant was recovered and loaded onto a 10−40% sucrose gradient made in 50 mM NaP pH 7 buffer, which was centrifuged for 6 h at 25 000 rpm using a SW-27 swinging bucket rotor in a Beckman ultracentrifuge. After centrifuging, the gradients were visualized in a dark room with the sucrose solution illuminated from above with an LED light: typically, a dense band in the middle of the gradient is observed, corresponding to VLPs. This band was collected and spun down using a Beckman 70Ti rotor at 40 000 rpm and 6 °C for approximately 2 h. The clear pellet was resuspended in buffer and assayed for quantity and purity of the VLPs. Note that pure (unmodified) VLPs typically yield a clear pellet; if a yellow tint was observed, the sucrose gradient and subsequent pelleting steps were repeated.

Synthetic Protocols. *Synthesis of 1.* 0.25 g (1.26 mmol) of 2-(bromomethyl)-2-(hydroxymethyl)-1,3-propanediol (**1a**) and 0.15 g (2.31 mmol) of sodium azide were dissolved in anhydrous DMF and refluxed at 120 °C for 24 h. The reaction was then concentrated under reduced pressure and the residue taken up in THF. The suspension was filtered to remove excess sodium azide. The filtrate was then again concentrated, the THF wash repeated, and the filtrate finally concentrated to yield **1b** as a straw-yellow oil. The product was confirmed using IR (azide stretch at 2100 cm^{-1}) and NMR (singlets at 3.25 and 3.45 ppm in D_2O, integrate 1:3, respectively).

Persulfation was achieved using pyridine-sulfur trioxide, which was repurified before every reaction by washing as follows. The powder was placed in a fritted glass funnel and first washed using ice-cold distilled water until the pH of the filtrate reached ∼5−6. The powder was then dried by washing sequentially with cold ethanol, dichloromethane, and finally diethyl ether. The final purified reagent is a white powder which is fluffy upon drying thoroughly; this was used immediately for sulfation. In an oven-dried flask 0.1 g of **1b** (0.6 mmol) and 1 g of purified pyridine−sulfur trioxide (6 mmol) were dissolved in anhydrous pyridine, and the mixture was left to stir at 60−70 °C for 4 h. The reaction was then concentrated under reduced pressure, followed by dilution with 30 mL of distilled water. The mixture was placed on ice: to the solution 5% aqueous NaOH was added dropwise until the pH of the solution reached approximately 9. The mixture was then concentrated under reduced pressure to yield a tan-yellow solid (**1**), characterized using IR (azide stretch at 2100 cm^{-1} and sulfate stretch at 1200−1300 cm^{-1}), NMR (singlets at 3.45 and 3.90 ppm in D_2O, integrate 1:3), and ESI-MS in negative ion mode ($[M\text{-}Na]^-$, calc 444.3, found 443.7). To account for any residual salt in the final preparation, the quantity of product in the mixture was quantified by NMR using 5 μL of added pyridine as an internal standard.

Synthesis of 2. 0.722 mL 6-bromo hexanol (**2a**; 1.0 g, 5.5 mmol) and 2.87 g sodium azide (44 mmol) were combined in anhydrous DMF overnight at 120 °C. The reaction was then concentrated under reduced pressure and resuspended in water. Hexanes were used to extract the organic product, which was washed several times with brine. The organic layer was then dried and concentrated under reduced pressure to yield **2b**. The product was confirmed using IR (azide stretch at 2096 cm^{-1}) and ^1H NMR ($CDCl_3$, 300 MHz): 1.46 ppm (4H, m), 1.64 ppm (4H, m), 3.27 ppm (2H, t), 3.65 ppm (2H, t).

Sulfation was achieved by adding 3.5 g (22 mmol) of purified pyridine sulfur trioxide (see purification protocol above) to a stirred solution of **2b** (0.3g, 2 mmol) in pyridine for 4 h at 60−

70 °C. The solvent was evaporated under reduced pressure and the reaction resuspended in a minimal amount of water. Following cooling of the mixture on ice, concentrated sodium hydroxide was added until a pH of ~9 was reached to generate the sodium salt. The remaining pyridine was extracted with heptanes and the aqueous layer concentrated under reduced pressure to provide **2**. IR stretches at 2100 and 1200 cm^{-1} were observed for the azide and sulfate, respectively. ^1H NMR (D_2O, 300 MHz): 1.45 ppm (4H, m), 1.60 ppm (2H, m), 1.70 ppm (2H, m), 3.35 ppm (2H, t), 4.12 ppm (2H, t). ESI-MS in negative ion mode $[M\text{-}Na]^-$: calc 222.3, found 221.9. As for **1**, quantification was by NMR with pyridine.

Bioconjugation. Lysine side chains on the surface of Qβ were first converted to alkyne moieties. To a 1275 μL solution of VLP in 0.1 M NaP pH 7 buffer, 145 μL of DMSO were added followed by 80 μL of a 444 mM stock of **3** in DMSO for final concentrations of 15% DMSO and 2 mg/mL VLP. The reaction was left to mix gently on a rotator overnight at room temperature. The mixture was then ultracentrifuged (Beckman 70Ti rotor, 40 000 rpm for 1 h at 6 °C) to pellet the VLP, which was then resuspended in NaP pH 7 buffer.

CuAAC reactions were performed as described by Hong, optimized for the reactions herein.[52] Buffers were bubble-degassed, and reactions were set up in a spherical argon-filled chamber ("glove globe") to reduce the oxygen content of the reaction. For each CuAAC reaction, the following reagents were added in this order, with the final volume made up to 1.5 mL using NaP pH 7 buffer: 2 mg of Qβ modified with **3** in 0.1 M NaP pH 7 buffer (1305 μL total), approximately 40 mM of **1** or **2** from aqueous stock solutions, a 45 μL mixture that contained 15 μL of 20 mM $CuSO_4$ and 30 μL of 50 mM THPTA, 75 μL of 100 mM aminoguanidine, and 75 μL of 100 mM sodium ascorbate in water. The reactions were allowed to mix on a rotator overnight on the benchtop, followed by ultracentrifugation to pellet the particles which were then resuspended in HBS buffer (50 mM HEPES, 100 mM NaCl, pH 7.4). CuAAC reaction of 6-carboxyfluorescein-TEG azide (Berry and Associates, FF 6110) was performed similarly: 5.8 mg were dissolved in 50 μL of DMSO and added to the reaction in place of **1** or **2**.

MALDI-MS Analysis. Approximately 50 μg of VLP were denatured in 100−150 μL of a solution containing 6−8 M urea and 50 mM dithiothreitol at 37 °C for 1 h. The reactions were then cleaned with C18 reverse-phase ZipTips (Millipore) according to the manufacturer using the following solutions made with Milli-Q water: equilibration solution 0.2% TFA, wash solution 0.1% TFA/5% methanol, elution solution 0.1% TFA/65% acetonitrile, wetting solution 50% acetonitrile. The final elution volume was 5 μL. Matrix solutions for MALDI-MS were made by saturating a 50% acetonitrile/0.1% TFA solution with sinapinic acid.

SDS-PAGE. Electrophoresis was performed using the XCell SureLock Mini-Cell, NuPage 4−12% bis-Tris 12-well gels, and staining with the ruthenium-based fluorescent SYPRO stain according to the manufacturer (Life Technologies). For quantification by gel, a BSA ladder was made using a 2 mg/mL standard solution (Pierce) with quantities ranging from 80 to 1000 ng loaded into each lane. Quantification was achieved by visualizing the gel under UV light and integrating the observed intensities using a UVP workstation with LabWorks software.

APTT Assay. Clotting assays were performed using the Stago STart 4 hemostasis analyzer. The desired amount of VLP (and protamine if required) in HBS buffer was diluted to a volume of 55 μL with HBS buffer. This solution was placed into the reaction cell along with 40 μL of normal human plasma (George King Biomedical), and 50 μL of Platelin (TriniCLOT from Tcoag). The cell was placed into the analyzer set at 37 °C and allowed to incubate for 3 min. Clotting was then initiated by adding 10 μL of 100 mM $CaCl_2$ in HBS, and the clotting time was recorded. Reaction times beyond 130 s were highly irreproducible, thus concentrations were chosen to keep clotting times under this value.

HEPtest Assay. The HEPtest kit was purchased from Sekisui Diagnostics and the assay was performed according to the manufacturer's instructions, with the following modifications. Samples consisted of 50 μL VLP or heparin solution in HBS buffer, 50 μL of normal human plasma, and 100 μL of FXa solution; the mixture was allowed to incubate at 37 °C for 2 min. 100 μL of RECALMIX were added to initiate clotting. Assays were performed with the Stago STart 4 hemostasis analyzer.

Complement Assay. The MicroVue SC5b-9 Plus EIA kit (Quidel, 96-well format) was used to assay for complement activation following the manufacturer's protocol. Samples consisted of 5 μL of normal human plasma, and a volume of VLP in HBS buffer that amounted to the desired mass of added VLP. After incubating the samples at 37 °C for 30 min, the solutions were diluted to 100 μL using the Specimen Diluent supplied with the kit; the entire 100 μL were applied to the wells of the plate. Absorption measurements were read at 450 nm with a 96-well plate reader (Biotek ELx50), which was also used to perform the washing steps. Terminal complement complex (TCC) concentrations were calculated based on a linear fit of the standard curve generated using the standards supplied with the kit. Data points represent at least duplicate measurements and are plotted as TCC concentration relative to that observed in the absence of VLP (a blank sample containing only buffer).

■ ASSOCIATED CONTENT

Supporting Information

ESI-MS, IR, and NMR spectra for ligands **1** and **2**; Qβ solvent-accessibility profile; MALDI-MS data for the VLP-fluorescein construct; size-exclusion FPLC of VLP conjugates; APTT data with protamine; HEPtest data. This material is available free of charge via the Internet at http://pubs.acs.org.

■ AUTHOR INFORMATION

Corresponding Author

*E-mail: udit@oxy.edu. Phone: 626-259-2761.

Notes

The authors declare no competing financial interest.

■ ACKNOWLEDGMENTS

This work was supported by the Research Corporation (Cottrell grant to A.K.U.), The Camille and Henry Dreyfus Foundation (startup grant to A.K.U.), and The Howard Hughes Medical Institute (undergraduate education grant to Occidental College). We thank Dr. Weidong Wang (Occidental College) for helpful discussions, Dr. Young In Oh (Caltech) and Dr. Vito Ferro (University of Queensland) for assistance with synthetic protocols, and Kristi Geiger (Occidental College) for assistance with ELISA.

■ ABBREVIATIONS

GAG, glycosaminoglycan; UFH, unfractionated heparin; FXa, Factor Xa; AT, antithrombin; LMWH, low molecular weight heparin; ULMWH, ultralow molecular weight heparin; HBS, HEPES-buffered saline; NaP, sodium phosphate; VLP, virus-like particle

■ REFERENCES

(1) Capila, I., and Linhardt, R. J. (2002) Heparin-protein interactions. *Angew. Chem., Int. Ed. 41*, 390−412.

(2) Garg, H. G., Linhardt, R. J., and Hales, C. A., Eds. (2005) *Chemistry and Biology of Heparin and Heparan Sulfate*, Elsevier, London.

(3) Linhardt, R. J., and Gunay, N. S. (1999) Production and chemical processing of low molecular weight heparins. *Semin. Thromb. Hemostasis. 25*, 5−16.

(4) *Heparin for drug and medical device use: monitoring crude heparin for quality* (2013) Food And Drug Administration, Department of Health and Human Services.

(5) Barrowcliffe, T. W. (2012) History of heparin. In *Heparin - A Centruy of Progress*, (Lever, R., Mulloy, B., and Page, C. P., Eds.) pp 3−22, Springer-Verlag, Berlin.

(6) Weitz, D., and Weitz, J. (2010) Update on heparin: what do we need to know? *J. Thromb. Thrombolysis 29*, 199−207.

(7) Sane, D. C. (2011) Unfractionated heparin: still going strong - despite limitations and evidence. *J. Invasive Cardiol. 23*, 13−18.

(8) Pike, R., Buckle, A., Le Bonniec, B., and Church, F. (2005) Control of the coagulation system by serpins. Getting by with a little help from glycosaminoglycans. *FEBS J. 272*, 4842−4851.

(9) Rosenberg, R., Armand, G., and Lam, L. (1978) Structure-function relationships of heparin species. *Proc. Natl. Acad. Sci. U.S.A. 75*, 3065−3069.

(10) Li, W., Johnson, D., Esmon, C., and Huntington, J. (2004) Structure of the antithrombin-thrombin-heparin ternary complex reveals the antithrombotic mechanism of heparin. *Nat. Struct. Mol. Biol. 11*, 857−862.

(11) Classen, D., Jaser, L., and Budnitz, D. (2010) Adverse drug events among hospitalized Medicare patients: epidemiology and national estimates from a new approach to surveillance. *Joint Commission Journal on Quality and Patient Safety 36*, 12−21.

(12) Pravinkumar, E., and Webster, N. R. (2003) HIT/HITT and alternative anticoagulation: current concepts. *Br. J. Anaesth. 90*, 676−685.

(13) Finley, A., and Greenberg, C. (2013) Heparin sensitivity and resistance: management during cardiopulmonary bypass. *Anesth. Analg. 116*, 1210−1222.

(14) Hirsh, J., Anand, S., Halperin, J., and Fuster, V. (2001) Guide to anticoagulant therapy: heparin: a statement for healthcare professionals from the American Heart Association. *Circulation 103*, 2994−3018.

(15) Liu, H., Zhang, Z., and Linhardt, R. J. (2009) Lessons learned from the contamination of heparin. *Nat. Prod. Rep. 26*, 313−321.

(16) Kishimoto, T., Viswanathan, K., Ganguly, T., Elankumaran, S., Smith, S., Pelzer, K., Lansing, J., Sriranganathan, N., Zhao, G., Galcheva-Gargova, Z., Al-Hakim, A., Bailey, G., Fraser, B., Roy, S., Rogers-Cotrone, T., Bushe, L., Whary, M., Fox, J., Nasr, M., Dal Pan, G., Shriver, Z., Langer, R., Nenkataraman, G., Austen, K., Woodcock, J., and Sasisekharan, R. (2008) Contaminated heparin associated with adverse clinical events and activation of the contact system. *New Eng. J. Med. 358*, 2457−2467.

(17) Gama, C. I., and Hsieh-Wilson, L. C. (2005) Chemical approaches to deciphering the glycosaminoglycan code. *Curr. Opin. Chem. Biol. 9*, 1−11.

(18) Volpi, N. (2006) Therapeutic applications of glycosaminoglycans. *Curr. Med. Chem. 13*, 1799−1810.

(19) Maxhimer, J. B., Quiros, R. M., Stewart, R., Dowlatshahi, K., Gattuso, P., Fan, M., Prinz, R. A., and Xu, X. L. (2002) Hepranase-1 expression is associated with the metastatic potential of breast cancer. *Surgery 132*, 326−333.

(20) Sasisekharan, R., Shriver, Z., Venkataraman, G., and Narayanasami, U. (2002) Roles of heparin-sulfate glycosaminoglycans in cancer. *Nat. Rev. Cancer 2*, 521−528.

(21) Iozzo, R. V., and San Antonio, J. D. (2001) Heparan sulfate proteoglycans: heavy hitters in the angiogenesis arena. *J. Clin. Invest. 108*, 349−355.

(22) Narita, K., Staub, J., Chien, J., Meyer, K., Bauer, M., Friedl, A., Ramakrishnan, S., and Shridhar, V. (2006) HSulf-1 inhibits angiogenesis and tumorigenesis in vivo. *Cancer Res. 66*, 6025−6032.

(23) Morimoto-Tomita, M., Uchimura, K., and Bistrup, A. (2005) Sulf-2, a proangiogenic heparan sulfate endosulfatase, is up-regulated in breast cancer. *Neoplasia 7*, 1001−1010.

(24) Cosmi, B., and Palareti, G. (2012) Old and new heparins. *Thromb. Res. 129*, 388−391.

(25) Schulman, S. (2014) Advantages and limitations of the new anticoagulants. *J. Intern. Med. 275*, 1−11.

(26) Levi, M. (2009) Emergency reversal of antithrombotic treatment. *Int. Emerg. Med. 4*, 137−145.

(27) Drahl, C. (2010) Anticoagulants in the pipeline may overcome the drawbacks of well-entrenched drugs. *Chem. Eng. News 88*, 15−22.

(28) Linkins, L.-A., and Weitz, J. I. (2010) New and emerging anticoagulant therapies for venous thromboembolism. *Current Treatment Options in Cardiovascular Medicine 12*, 142−155.

(29) Schulman, S., and Bijsteervald, N. (2007) Anticoagulants and their reversal. *Transfus. Med. Rev. 21*, 37−48.

(30) Hull, R. D., and Townshend, G. (2013) Long-term treatment of deep-vein thrombosis with low-molecular-weight heparin: An update of the evidence. *Thromb. Hemostasis 110*, 14−22.

(31) Holzheimer, R. G. (2004) Low-molecular-weight heparin (LMWH) in the treatment of thrombosis. *Eur. J. Med. Res. 9*, 225−239.

(32) Constantino, G., Ceriani, E., Rusconi, A. M., Podda, G. M., Montano, N., Duca, P., Cattaneo, M., and XCasazza, G. (2012) Bleeding risk during treatment of acute thrombotic events with subcutaneous LMWH compared to intravenous unfractionated heparin; a systematic review. *PLoS One 7*, 1−10.

(33) Dulaney, S. B., and Huang, X. (2012) Strategies in synthesis of heparin/heparin sulfate oligosaccharides: 2000-present. *Adv. Carbohydr. Chem. Biochem.*, 95−136.

(34) Rouet, V., Meddahi-Pelle, A., Miao, H.-Q., Vlodavsky, I., Caruelle, J.-P., and Barritault, D. (2006) Heparin-like synthetic polymers, named RGTAs, mimic biological effects of heparin in vitro. *J. Biomed. Mater. Res., Part A 78a*, 792−797.

(35) Freeman, C., Liu, L., Banwell, M. G., Brown, K. J., Bezos, A., Ferro, V., and Parish, C. R. (2006) Use of sulfated linked cyclitols as heparan sulfate mimetics to probe the heparin/heparan sulfate binding specificity of proteins. *J. Biol. Chem. 208*, 8842−8849.

(36) Lu, L.-D., Shie, C.-R., Kulkarni, S. S., Pan, G.-R., Lu, X. A., and Hung, S.-C. (2006) Synthesis of 48 disaccharide building blocks for the assembly of a heparin and heparan sulfate oligosaccharide library. *Org. Lett. 8*, 5995−5998.

(37) Cao, H. Z., and TYu, B. (2005) Synthesis of a S-linked heparan sulfate trisaccharide as the substrate mimic of heparanase. *Tetrahedron Lett. 46*, 4337−4340.

(38) Polat, T., and Wong, C.-H. (2007) Anomeric reactivity-based one-pot synthesis of heparin-like oligosaccharides. *J. Am. Chem. Soc. 129*, 12795−12800.

(39) Petitou, M., Jacquinet, J.-C., Sinay, P., Choay, J., Lormeau, J. C., and Nassr, M. (1989) *Process for the organic synthesis of oligosaccharides and derivatives thereof*, U. S. Patent 4,818,816.

(40) Seifert, J., Singh, L., Ramsdale, T. E., West, M. L., and Drinnan, N. B. (2009) *Synthetic heparin pentasaccharides*, U. S. Patent 7,541,445B2.

(41) Lin, F., Lian, G., and Zhou, Y. (2013) Synthesis of fondaparinux: modular synthesis investigation for heparin synthesis. *Carb. Res. 371*, 32−39.

(42) Xu, Y., Masuko, S., Takieddin, M., Xu, H., Liu, R., Jing, J., Mousa, S. A., Linhardt, R. J., and Liu, J. (2011) Chemoenzymatic

synthesis of homogeneous ultralow molecular weight heparins. *Science 334*, 498−501.
(43) Bhaskar, U., Sterner, E., Hickey, A. M., Onishi, A., Zhang, F. M., Dordick, J. S., and Linhardt, R. J. (2012) Engineering of routes to heparin and related polysaccharides. *Appl. Microbiol. Biotechnol. 93*, 1−16.
(44) Golmohammadi, R., Fridborg, K., Maija, B., Valegard, K., and Liljas, L. (1996) The crystal structure of bacteriophage Qβ at 3.5 A resolution. *Structure 4*, 543−554.
(45) Astronomo, R. D., Kaltgrad, E., Udit, A. K., Wang, S. K., Doores, K. J., Huang, C. Y., Pantophlet, R., Paulson, J. C., Wong, C. H., Finn, M. G., and Burton, D. R. (2010) Defining criteria for oligomannose immunogens for HIV using icosahedral virus capsid scaffolds. *Chem. Biol. 17*, 357−370.
(46) Udit, A. K., Everett, C., Gale, A. J., Reiber-Kyle, J., Ozkan, M., and Finn, M. G. (2009) Heparin antagonism by polyvalent display of cationic motifs on virus-like particles. *ChemBioChem 10*, 503−510.
(47) Prasuhn, D. E., Jr., Yeh, R. M., Obenaus, A., Manchester, M., and Finn, M. G. (2007) Viral MRI contrast agents: coordination of gd by native virions and attachment of Gd complexes by azide-alkyne cycloaddition. *Chem. Commun.*, 1269−1271.
(48) Kaltgrad, E., Sen Gupta, S., Punna, S., Huang, C.-Y., Chang, A., Wong, C.-H., Finn, M. G., and Blixt, O. (2007) Anti-carbohydrate antibodies elicited by polyvalent display on a viral scaffold. *ChemBioChem 9*, 1455−1462.
(49) Pokorski, J. K., Hovlid, M. L., and Finn, M. G. (2011) Cell targeting with hybrid Qb virus-like particles displaying epidermal growth factor. *ChemBioChem 12*, 2441−2447.
(50) Rhee, J.-K., Baksh, M., Nycholat, C., Paulson, J. C., Kitagishi, H., and Finn, M. G. (2012) Glycan-targeted virus-like nanoparticles for photodynamic therapy. *Biomacromolecules 13*, 2333−2338.
(51) Gale, A. J., Elias, D. J., Averell, P. M., Teirstein, P. S., Buck, M., Brown, S. D., Polonskaya, Z., Udit, A. K., and Finn, M. G. (2011) Engineered virus-like nanoparticles reverse heparin anticoagulation more consistently than protamine in plasma from heparin-treated patients. *Thromb. Res. 128*, e9−e13.
(52) Hong, V., Presolski, S., Ma, C., and Finn, M. (2009) Analysis and optimzation of copper-catalyzed azide-alkyne cycloaddition for bioconjugation. *Angew. Chem., Int. Ed. 48*, 9879−9883.
(53) Hong, V., Udit, A. K., Evans, R., and Finn, M. G. (2008) Electrochemically protected copper(I)-catalyzed azide-alkyne cycloaddition. *ChemBioChem 9*, 1481−1486.
(54) Gupta, S. S., Kuzelka, J., Singh, P., Lewis, W. G., Manchester, M., and Finn, M. G. (2005) Accelerated bioorthogonal conjugation: a practical method for the ligation of diverse functional molecules to a polyvalent virus scaffold. *Bioconjugate Chem. 16*, 1572−1579.
(55) Bink, H. H. J., and Pleij, C. W. A. (2002) RNA-protein interactions in spherical viruses. *Arch. Virol. 147*, 2261−2279.
(56) Lim, F., Spingola, M., and Peabody, D. S. (1996) The RNA-binding site of bacteriophage Qb coat protein. *J. Biol. Chem. 13*, 31839−31845.
(57) Horn, W. T., Tars, K., Grahn, E., Heigstrand, C., Baron, A. J., Lago, H., Adams, C. J., Peabody, D. S., Phillips, S. E. V., Stonehouse, N. J., Liljas, L., and Stockley, P. G. (2006) Structural basis of RNA binding discrimination between bacteriophages Q beta and MS2. *Structure 14*, 487−495.
(58) Strable, E., Prasuhn, D. E., Jr., Udit, A. K., Brown, S. D., Link, A. J., Ngo, J. T., Lander, G., Quispe, J., Potter, C. S., Carragher, B., Tirrell, D. A., and Finn, M. G. (2008) Unnatural amino acid incorporaton into virus-like particles. *Bioconjugate Chem. 19*, 866−875.
(59) Fiedler, J., Higginson, C., Hovlid, M., Kishlukin, A., Castillejos, A., Manzenrieder, F., Campbell, M., Voss, N., Potter, C., Carragher, B., and Finn, M. (2012) Engineered mutations change the structure and stability of a virus-like particle. *Biomacromolecules 13*, 2339−2348.
(60) Velders, A. J., and Wildevuur, C. R. H. (1986) Platelet damage by protamine and the protective effect of prostacyclin: an experimental study in dogs. *Ann. Thorac. Surg. 42*, 168−171.
(61) Cobel-Geard, R. J., and Hassouna, H. I. (1983) Interaction of Protamine sulfate with thrombin. *Am. J. Hematol. 14*, 227−233.
(62) Salvador-Morales, C., and Sim, R. B. (2013) Complement activation. In *Handbook of immunological properties of engineered nanomaterials* (Dobrovolskaia, M. A., and McNeil, S., Eds.) pp 357−384, World Scientific Publishing Co., Singapore.
(63) Edens, R. E., Linhardt, R. J., and Weiler, J. M. (1993) Heparin is not just an anticoagulant anymore: six and one-half decades of studies on the ability of heparin to regulate complement activity. In *Complement Today* (Cruise, J. M., and Lewis, R. E., Eds.) pp 96−120, Karger, Basel.
(64) van den Hoven, J. M., Nemes, R., Metselaar, J. M., Nuijen, B., Beijnen, J. H., Storm, G., and Szebeni, J. (2013) Complement activation by PEGylated liposomes containing prednisolone. *Eur. J. Pharm. Sci. 49*, 265−271.
(65) Ikeda, Y., Charef, S., Ouidja, M.-O., Bearbier-chassefiere, V., Sineriz, F., Duchesnay, A., Narasimprakash, H., Martelly, I., Kern, P., Barritault, D., Petit, E., and Papy-Garcia, D. (2011) Synthesis and biological activities of a library of glycosaminogylcans mimetic oligosaccharides. *Biomaterials 32*, 769−776.
(66) Sangaj, N., Kyriakakis, P., Yang, D., Chang, C.-W., Arya, G., and Varghese, S. (2010) Heparin mimicking polymer promotes myogenic differentiation of muscle progenitor cells. *Biomacromolecules 11*, 3294−3300.
(67) de Paz, J. L., Noti, C., Bohm, F., Werner, S., and Seeberger, P. H. (2007) Potentiation of fibroblast growth factor activity by synthetic heparin oligosaccharide glycodendrimers. *Chem. Biol. 17*, 879−887.
(68) Turk, H., Haag, R., and Alban, S. (2004) Dendritic polyglycerol sulfates as new heparin analogues and potent inhibitors of the complement system. *Bioconjugate Chem. 15*, 162−167.
(69) Prasuhn, D. E., Jr., Kuzelka, J., Strable, E., Udit, A. K., Cho, S.-H., Lander, G. C., Quispe, J. D., Diers, J. R., Bocian, D. F., Potter, C., Carragher, B., and Finn, M. G. (2008) Polyvalent display of heme on hepatitis B virus capsid protein through coordination to hexahistidine tags. *Chem. Biol. 15*, 513−519.
(70) Studier, F. W. (2005) Protein production by auto-induction in high-density shaking cultures. *Protein Expression Purif. 41*, 207−234.